Chemistry & Biology
Brief Communication

A Peptidomimetic Approach to Targeting Pre-amyloidogenic States in Type II Diabetes

James A. Hebda,[1,3] Ishu Saraogi,[2,3] Mazin Magzoub,[1] Andrew D. Hamilton,[1,2,*] and Andrew D. Miranker[1,*]
[1]Department of Molecular Biophysics and Biochemistry, Yale University, 260 Whitney Avenue, New Haven, CT 06520-8114, USA
[2]Department of Chemistry, Yale University, 225 Prospect Street, P.O. Box 208107, New Haven, CT 06520-8107, USA
[3]These authors contributed equally to this work
*Correspondence: andrew.miranker@yale.edu (A.D.M.), andrew.hamilton@yale.edu (A.D.H.)
DOI 10.1016/j.chembiol.2009.08.013

SUMMARY

Protein fiber formation is associated with diseases ranging from Alzheimer's to type II diabetes. For many systems, including islet amyloid polypeptide (IAPP) from type II diabetes, fibrillogenesis can be catalyzed by lipid bilayers. Paradoxically, amyloid fibers are β sheet rich while membrane-stabilized states are α-helical. Here, a small molecule α helix mimetic, IS5, is shown to inhibit bilayer catalysis of fibrillogenesis and to rescue IAPP-induced toxicity in cell culture. Importantly, IAPP:IS5 interactions localize to the putative α-helical region of IAPP, revealing that α-helical states are on pathway to fiber formation. IAPP is not normally amyloidogenic as its cosecreted partner, insulin, prevents self-assembly. Here, we show that IS5 inhibition is synergistic with insulin. IS5 therefore represents a new approach to amyloid inhibition as the target is an assembly intermediate that may additionally restore functional IAPP expression.

INTRODUCTION

Type II diabetes is an increasingly prevalent disease characterized by the loss of blood glucose homeostasis and systemic insulin resistance. The consequences of diabetes are far reaching, resulting in greatly increased risks of heart disease, kidney damage, and circulatory problems. The current epidemic of obesity in the United States and Europe is expected to increase the prevalence of diabetes in children as well as adults (Pontiroli, 2004). It is therefore of great importance to understand the causes and factors implicated in diabetic pathology. One unique feature of the pathology is the formation of proteinaceous plaques in the endocrine pancreas (Haataja et al., 2008; Hoppener et al., 2000; Kahn et al., 1999). These amyloid plaques are composed primarily of fibers formed from islet amyloid polypeptide (IAPP). Fiber formation is a widespread phenomenon in a number of other important diseases such as Alzheimer's in which the Aβ peptide aggregates to form amyloid plaques (Finder and Glockshuber, 2007).

The misfolding and self-assembly of IAPP into fibers is correlated with the loss of insulin secreting β cells. IAPP is a 37 amino acid, natively unstructured peptide hormone that is copackaged with insulin in the secretory granules of the β cells (Clark and Nilsson, 2004; Hull et al., 2004). In addition, insulin and IAPP demonstrate coregulated expression and are coprocessed by a common convertase (Badman et al., 1996). As a hormone, many activities have been attributed to IAPP, ranging from regulation of gastric emptying to paracrine/autocrine feedback (Cooper, 1994; Hay et al., 2004). The latter is evident in the fact that transgenic human IAPP (hIAPP) rats have defective insulin secretion profiles (Matveyenko and Butler, 2006a). In addition, insulin likely plays an important role in preventing IAPP aggregation in vivo, as insulin is a potent inhibitor of IAPP aggregation in vitro (Larson and Miranker, 2004). The link between IAPP amyloid and disease states (Porte and Kahn, 2001; Marzban et al., 2003) has been supported recently by transgenic rat models for type II diabetes (Matveyenko and Butler, 2006b). Rat IAPP (rIAPP) does not readily aggregate in vitro and rats do not spontaneously develop type II diabetes. In contrast, rodents transgenic for hIAPP develop symptoms similar to type II diabetes. A notable example among these is the HIP rat, which closely follows the human progression of diabetes, including systemic insulin resistance, elevated glucose levels, and loss of β cell mass (Matveyenko and Butler, 2006a). These findings have clearly linked IAPP misfolding to β cell death and increased pathogenicity in type II diabetes.

Amyloid proteins misfold and aggregate into highly ordered fibrous structures. These are characterized by the noncovalent assembly of β strands. These strands form sets of two or more β sheets that run the entire length of a fiber (Tycko, 2006). Such states are highly stable, often demonstrating strong resistance to chemical and proteolytic degradation. The assembly pathway of amyloid is that of a nucleation-dependent polymerization (Frieden, 2007; Powers and Powers, 2008; Ruschak and Miranker, 2007). Nucleation-dependent polymerization is characterized by kinetic profiles beginning with a lag phase, where no detectable fiber is generated. Nucleation represents the initial formation of states that are competent to elongate. This results in an apparently cooperative kinetic transition to the final amyloid state. Such systems effectively behave like 1D crystals with the nucleation processes bypassable by seeding with the addition of preformed fibers (Harper and Lansbury, 1997).

The crystal-like propagation properties of fibers have been widely capitalized on to identify inhibitors based on crystal poisoning. In this approach, inhibitors are designed to possess sufficient structure to bind fiber ends. Once bound, further addition of precursor is prohibited. Early examples of this for Alzheimer's disease include modified variants of a subpeptide,

LVFFA, of $A\beta_{42}$ (Findeis et al., 2001). For IAPP, such approaches include not only subpeptides but also full-length IAPP in which the backbone amide has been methylated (Yan et al., 2006) and nonamyloidogenic point mutations (Abedini et al., 2007). An alternative approach has been to identify small molecules that interfere with assembly. For example, a lead compound, DAPH, has been shown to inhibit Aβ amyloid aggregation and toxicity (Wang et al., 2008). Like DAPH, many of these compounds are polycyclic (Aitken et al., 2003; LeVine, 2007) or polyphenolic (Porat et al., 2006; Bastianetto et al., 2008). It has been proposed that the majority of these compounds act by intercalating between β strands or β sheets, disrupting intermediate and fiber state interactions (Porat et al., 2004, 2006). Recently, several polycyclic compounds that bind α-synuclein have been shown by nuclear magnetic resonance (NMR) to bind to the same subset of residues, further suggesting a common molecular basis for their inhibition of amyloid formation (Rao et al., 2008).

The fiber state represents the product of amyloidogenesis; however, it is the intermediates of amyloid formation that represent the toxic species (Lashuel and Lansbury, 2006; Hebda and Miranker, 2009). This has long been conjectured as a result of the poor correlation between amyloid burden and disease pathology such as dementia in Alzheimer's. The current paradigm is that toxicity is mediated by intermediate oligomeric states that act by permeabilizing lipid bilayers. Oligomers bound to cellular membranes have been visualized using oligomer-specific antibodies in a number of amyloid systems (Gong et al., 2003; Kayed et al., 2004). In our own work, we determined that IAPP can bind to lipid bilayers to form monodisperse and heterogeneous oligomeric populations (Knight et al., 2006). Remarkably, both states are predominantly α-helical with the latter having a high capacity to render model membranes permeable to cations and small molecules. These oligomeric states were also best correlated to efficient catalysis of fiber formation. The α-helical region of IAPP has been mapped to an ~20 residue subdomain (see Figures 1B and 1C). When synthesized as a separate peptide, $IAPP_{1\text{-}19}$ can bind to membranes and adopt an α-helical, membrane-permeabilizing state, but does not progress to form amyloid (Brender et al., 2008). We hypothesize that membrane-bound α-helical oligomers represent the toxic species and are on pathway to amyloid formation. Toward that end, we have screened amyloid inhibitors that have been rationally designed to interact with α-helical states. This design strategy (Saraogi and Hamilton, 2008) has here enabled a kinetic and structural elucidation of the role of α-helical states in affecting the IAPP disorder to amyloid transition.

RESULTS

In this work, a synthetic, α-helical protein mimetic scaffold is used to probe IAPP fiber formation. The IS scaffold is particularly relevant to IAPP and possibly other amyloid peptides (such as $A\beta_{42}$ and α-synuclein) as these systems sample α-helical states as part of the amyloid formation process (Hebda and Miranker, 2009). The IS scaffold is organized so as to facially project functional groups at i, i + 3 (or i + 4), i + 7… spacings. A number of compounds have recently been assayed for their effects on IAPP fiber formation (Saraogi et al., 2009). Here, we have selected a pentameric IS compound that presents five carboxylates, IS5 (Figure 1A), for detailed study. Specifically, we study the effect of IS5 on the kinetics of fiber formation in solution, as catalyzed by lipid bilayer surfaces, in seeded elongation assays and in ternary reactions with a cosecreted hormone, insulin. Kinetic effects are compared to structural measurements using 1D and 2D NMR. Our goal is to probe the mechanism of amyloid fiber assembly and to relate mechanistic information to possible pharmacological strategies.

Nucleation of IAPP fiber formation is accelerated by addition of IS5. Fiber formation reactions were conducted in 96 well plates using the fluorescence of thioflavin T (ThT) as an indicator of amyloid assembly. Briefly, reactions are initiated by dilution of a DMSO stock of IAPP into buffer (pH 7.4; 50 mM phosphate and 100 mM KCl) at 25°C. Fiber formation was monitored using the time-dependent change in the fluorescence intensity of ThT (LeVine, 2007). IAPP gives nucleation-dependent kinetic profiles characterized, in part, by sigmoidal shape (Figure 2). Kinetic rates are characterized from these profiles using the reaction midpoint, or t_{50}. Due to effects of IS5 interfering with ThT intensity, the t_{50} and not absolute intensity was used as an indicator of IS5's effects on fiber formation reactions. The t_{50} were obtained by fitting the kinetic traces to a sigmoid (see Equation 1 in the Supplemental Experimental Procedures available online), with the inflection point of the curve taken as representing the reaction t_{50}.

Amyloid formation by IAPP in solution is accelerated by IS5 primarily as a result of changes to the rate of primary nucleation. This is suggested, in part, by the dramatic decrease in fiber formation lag time in the presence of IS5 (Figure 2A). Conduction of a 10 μM IAPP fiber formation reaction in the presence of 10 μM IS5 under standard solution conditions results in a t_{50} that is 0.18 ± 0.02 times as long as a control reaction in the absence of IS5 (3.6 ± 0.3 hr and 20.1 ± 0.6 hr, respectively). Intriguingly, the magnitude of this effect is still large (0.63 ± 0.03) even at 1 μM IS5 (data not shown). One possible origin for this effect is that IS5 acts on intermediates that form on the 3–4 hr time scale. In repeat experiments in which IS5 is instead added after 4 hr to an IS5-free reaction, a t_{50} of 8.1 ± 0.3 hr is observed (data not shown). In this case, the fiber formation reaction is occurring ~4 hr after contact with IS5. We conclude that IS5 does not act on late (3–4 hr) intermediate species. Rather, interactions occur with very early species and/or a monomeric precursor. That IS5 potently accelerates fiber formation is of mechanistic interest as the complex it forms appears to promote the initial nucleation of fibers.

This is further supported by the absence of an IS5 effect on seeded reaction kinetics. Seeded kinetics are collected by providing amyloid reactions with preformed fibers. Reaction profiles are typically exponential, as seeded fiber formation is driven predominantly by elongation. The presence of sigmoidal behavior in such reactions is a consequence of contributions from secondary nucleation processes, i.e., the fiber-dependent production of new fiber ends, such as might occur as a result of fiber breakage. Here, the t_{50} of a 20 μM IAPP reaction conducted in the presence of 4 μM of preformed fiber seed is 2.3 ± 0.2 hr (Figure 2B). The profile retains sigmoidal character and as the t_{50} is substantially less than the unseeded reaction t_{50}, this indicates the presence of both elongation and secondary

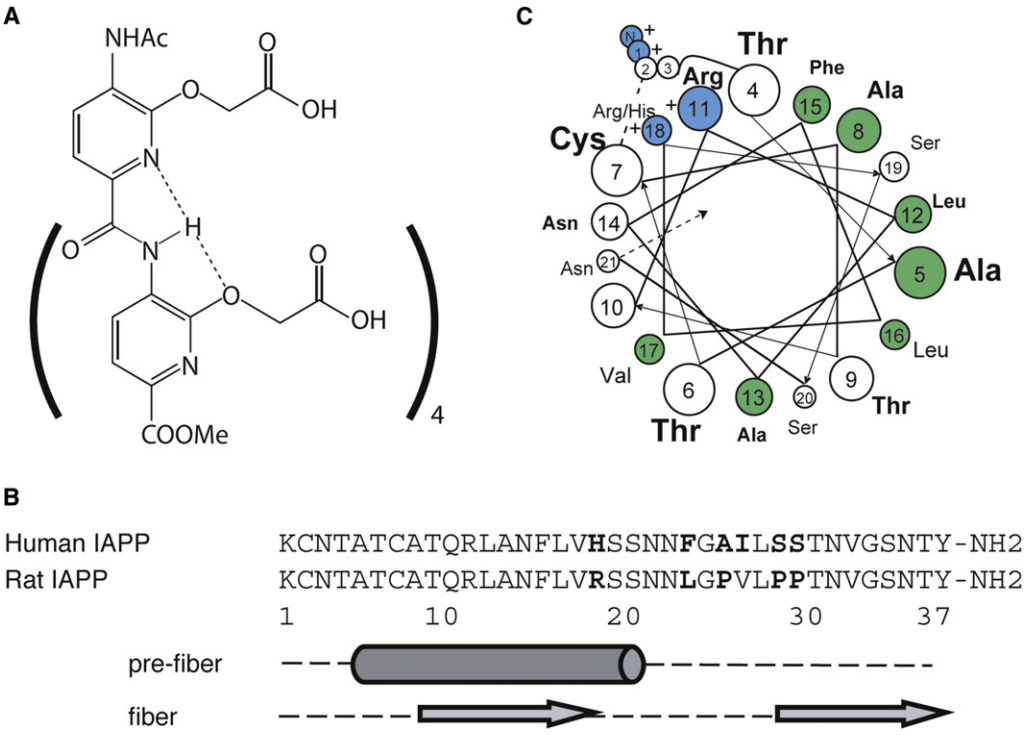

Figure 1. Structural Representations of IS5 and IAPP

(A) Structure of the helix mimetic compound IS5.

(B) Alignment of human and rat sequences of IAPP. Helical states sampled by both hIAPP and rIAPP in dilute solution and on membranes are indicated with a cylinder (Williamson and Miranker, 2007). β strands that were unambiguously determined by solid state NMR of hIAPP fibers are indicated with arrows (Luca et al., 2007).

(C) Helical wheel representation of residues 1–21. Polar residues are shown in white, charged in blue, and aliphatics in green. A disulfide between residues 2 and 7 is indicated with a dashed line.

nucleation processes, consistent with previous reports (Padrick and Miranker, 2002). Importantly, the addition of 20 μM IS5 to an otherwise identical reaction yields only mild inhibition, t_{50} = 2.8 ± 0.1 hr. Acceleration of solution phase reactions, but not seeded reactions, clearly shows that IS5 affects primary nucleation events. Neither elongation nor secondary nucleation processes represent targets of IS5.

IS5 acts as an inhibitor of lipid bilayer-catalyzed fiber formation. IAPP fiber formation is readily accelerated by lipid bilayers in a process associated with disease pathology (Hebda and Miranker, 2009). Here, we use a 1:1 mixture of 1,2-dioleoyl-*sn*-glycero-3-phosphocholine (DOPC) and 1,2-dioleoyl-*sn*-glycero-3-phospho-(1′-rac-gylcerol) (DOPG) lipids, extruded into 100 nm unilamellar vesicles as a reagent. At 10 μM IAPP and 630 μM lipid, the amyloid reaction t_{50} is 0.63 ± 0.01 hr (Figure 2C). Addition of IS5 at 10 μM to the former reaction conditions clearly results in inhibition giving a t_{50} of 2.1 ± 0.1 hr (Figure 2C). Like any ligand, the potency of IS5 will be affected by the structure and energetic details of its interaction with IAPP. At a molecular level, we note that IS5 is a polyanion with a calculated logP of −6.9 and is therefore unlikely to partition into a lipid bilayer. A compound with similar anionic character, diethylene triamine pentaacetic acid, showed no effects on lipid-catalyzed IAPP fiber formation (Saraogi et al., 2009). This suggests that IAPP:IS5 interactions have molecular specificity.

IS5 inhibits hIAPP-induced cytotoxicity. The effect of hIAPP on INS-1 cells, a well-characterized β cell model (Hohmeier et al., 2000), was assessed by the 3-(4,5-Dimethylthiazol-2-yl)-2,5-diphenyltetrazolium bromide (MTT) cell viability assay. hIAPP exhibited strong cytotoxic effects, with cell viability decreased to ~50% in the presence of 5 μM hIAPP and ~40% in the presence of 10 μM hIAPP (Figure 2D). IS5 significantly reduced the toxic effects of hIAPP, with complete rescue (i.e., 100% cell viability) observed at an IS5 to peptide ratio of 2:1. IS5 exhibited no intrinsic cytotoxicity up to 50 μM (data not shown). Melittin, from bee venom, was used as a positive control as its cytotoxicity is associated with a disordered to α-helix transition upon binding lipid bilayers. At 5 μM, melittin reduced cell viability by 98% and was not rescued even at ratios of 5:1 (IS5/melittin) (data not shown). This suggests that the amelioration of toxicity by IS5 is specific for structures formed by IAPP.

Solution phase interactions of IAPP with IS5 were determined by heteronuclear NMR. NMR spectra were collected using the sequence variant of IAPP from rats (rIAPP). rIAPP binds lipid bilayers with comparable properties to hIAPP, can disrupt membrane integrity, and yet does not readily form aggregates (Knight et al., 2006). IS5 was titrated from 0 to 475 μM into a sample containing 120 μM rIAPP at pH 6.5 and monitored by ^{1}H ^{15}N HSQC (Figures 3A and 3B and Figure S1). This pH was chosen to

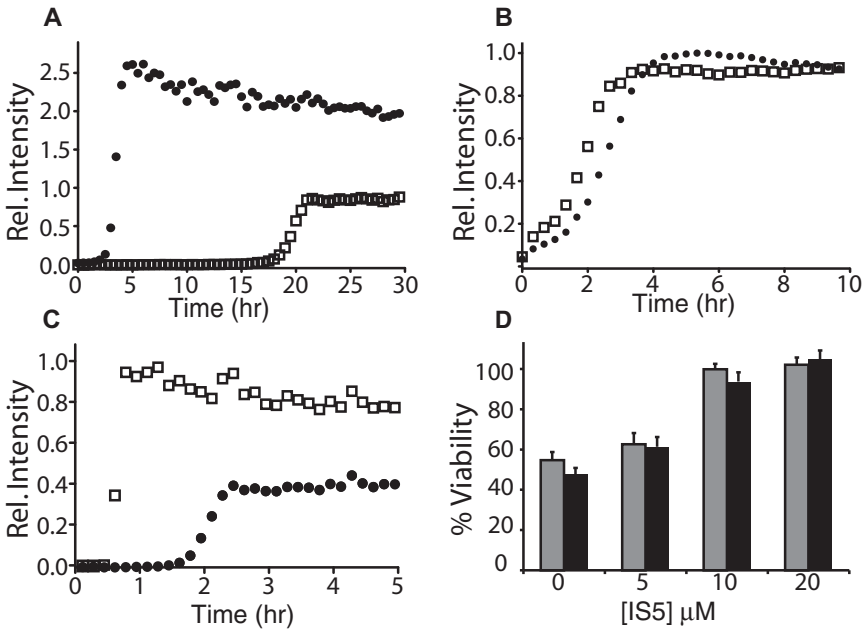

Figure 2. Effect of IS5 on the Kinetics of hIAPP Fiber Formation

Representative traces showing the effect of IS5 on de novo fiber formation in solution (A), on solution phase fiber formation seeded with preformed fibers (B), on de novo fiber formation catalyzed by a lipid bilayer (C), and on IAPP-induced cell toxicity (D).

(A–C) Reactions were performed in the presence (filled) and absence (open) of compound (1:1 IS5/IAPP). De novo reactions contained 10 μM hIAPP and 10 μM IS5. Seeded kinetics were performed at 20 μM hIAPP with the addition of 4 μM preformed IAPP fibers and 20 μM IS5. Lipid catalysis was performed by addition of 630 μM lipid in the form of a 1:1 mixture of DOPG/DOPC unilamellar liposomes.

(D) Inhibition of hIAPP cell toxicity by IS5. INS-1 cells were treated with hIAPP (5 μM [gray] or 10 μM [black]) and the indicated concentration of IS5. Cell viability was then assayed by MTT reduction (see Supplemental Experimental Procedures). Results are expressed as percentages of the control cells exposed only to a matched volume of neat DMSO. All experiments performed at least in triplicate. For (D), error bars represent SEM. For (A)–(C), statistics are quoted in the main text.

balance issues of solubility of IS5 and to minimize signal loss due to amide hydrogen exchange. The acceleration of hIAPP fiber formation by IS5 reported here at pH 7.4 is unaffected by this drop in pH (data not shown).

IS5 causes shifts of amide peaks within the helical domain of IAPP. Shifts were observed for all residues spanning 5 to 19. This region has previously been characterized by NMR as intrinsically disordered with a strong bias toward the sampling of α-helical states (Williamson and Miranker, 2007). No significant shifts were observed for residues 23–37 (Figure 3B). For example, serine 19 and 20 shift dramatically, whereas serine 34 is unaffected (Figure 3A). This trend of unchanged (C-terminal residues) versus shifted peaks (N-terminal residues) can clearly be noted between 0 μM and 475 μM IS5 (Figure 3B). Importantly, binding is nearing saturation at the highest concentrations of IS5 used (Figure S2). These binding data fit well to a single binding event ($R^2 > 0.97$) with an apparent binding affinity of 160 ± 20 μM. No shifts are apparent in control titrations using only DMSO (data not shown). The localization of perturbation to residues 5–19 of IAPP clearly implicates this region as the site of action of IS5. For hIAPP, it is possible that additional shifts could occur beyond residue 19, but these are prevented by the three proline residues present only in rIAPP. Thus, while it remains possible that the extent of IS5 interactions with hIAPP is greater than that observed in rIAPP, it is nevertheless clear that the helical region of IAPP is important to primary nucleation.

IS5 reduces the extent of IAPP binding to lipid bilayers. Binding of IAPP to liposomes can be measured with limited residue specificity using liposomes composed of 1:1 DOPG/DOPC and ^{1}H NMR (Figure 3C). Titrating rIAPP (with and without IS5) with increasing concentrations of liposomes clearly shows a diminishment of several peaks assignable to the helical region. Here, we highlight the aryl proton peaks of residue 15. In the absence of liposomes, the addition of IS5 to IAPP causes marked shifts to the aryl peaks of F15 (Figure 3C). In the absence of IS5, the peaks of F15 can readily be seen to broaden and lose intensity upon titration with liposomes (Figure 3C and Figure S3). Importantly, the extent of this signal loss is greatly diminished when equimolar IS5 is present. This observation can similarly be made directly as IS5 reduces the extent of cofloatation of rIAPP with liposomes upon centrifugation (Figure S3D). This suggests that IS5 is competing with the lipid surface for IAPP binding, thereby lowering the effective binding affinity of IAPP for the lipid surface.

The capacity of IS5 to act as inhibitor of lipid-catalyzed fiber formation is increased in the presence of insulin (Figure 4). We previously showed that insulin is a remarkably potent inhibitor of solution phase fiber formation (Larson and Miranker, 2004). Substoichiometric insulin readily inhibits solution phase IAPP fiber formation by greater than 10-fold. In marked contrast, we have recently shown that insulin is a weak inhibitor of lipid bilayer-catalyzed fiber formation (Knight et al., 2008). This observation led us to speculate that changes in lipid biochemistry might serve as a trigger for amyloid formation in type II diabetes (Knight and Miranker, 2004). What we characterize as weak inhibition by insulin is shown here in the context of the lipid catalysis of a 10 μM IAPP reaction (Figure 4). Addition of 5-fold molar excess of insulin to such a reaction results in a t_{50} that is 6.0 ± 0.4 times slower than the parent reaction. Importantly, whereas in the absence of insulin, 10 μM IS5 inhibits the lipid-catalyzed t_{50} by 2.3 ± 0.2-fold, in the presence of 50 μM insulin, 10 μM IS5 results in a t_{50} delayed by 15 ± 1.7-fold. This dramatic increase in inhibition is consistent with a model where pre-amyloidogenic forms of IAPP bound to lipid membranes are protected from insulin inhibition (Knight et al., 2008). Here, it appears that IS5 is able to compete IAPP off the lipid surface, increasing the accessibility of insulin to IAPP.

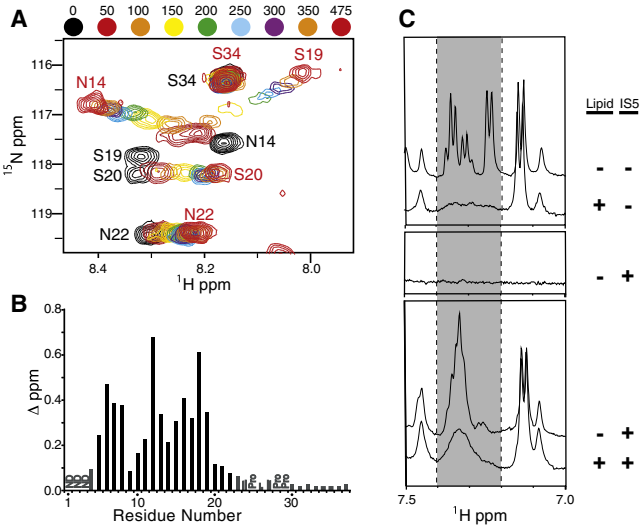

Figure 3. Structural Characterizations of IS5:IAPP Interactions

(A) Overlay of ^{1}H-^{15}N HSQC spectra of rIAPP showing shifts upon titration with IS5. A representative region of the full spectrum is shown with the indicated concentrations of IS5.

(B) Per residue Δ ppm between 0 and 475 μM IS5 showing the peak shifts within the helical region. Contributions from proton and nitrogen dimensions were combined and scaled as per Grzesiek et al. (1996). Peaks were not detected (ND) for residues 1–3, and prolines at residues 25, 28, and 29 result in no peaks (Pro). Residues 24, 26, and 27 have two assigned peaks (Williamson and Miranker, 2007), with each shown as separate values.

(C) Effect of IS5 on rIAPP lipid binding assessed by ^{1}H NMR signal loss of phenylalanine 15 (F15). Spectra of 150 μM rIAPP in the presence or absence of liposomes (1.25 mM lipid at 1:1 DOPG/DOPC) or in the presence or absence of 150 μM IS5 are indicated on right. Aryl protons of F15 in 1D ^{1}H spectra are indicated using a gray background. IS5 alone (middle spectrum) is shown to confirm that these effects are not due to signal overlap with the F15 peaks.

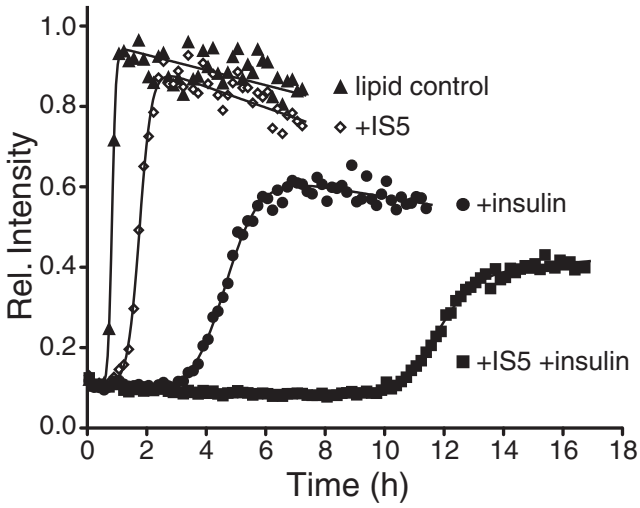

Figure 4. Synergy of Inhibition by IS5 and Insulin

Representative traces of IAPP amyloid formation kinetics conducted under lipid-catalyzed conditions (630 μM lipid at 1:1 DOPG/DOPC). Control lipid-catalyzed IAPP kinetics at 10 μM IAPP (triangles) are inhibited by addition of 10 μM IS5 (diamonds) or 50 μM insulin (circles). Simultaneous addition of both 10 μM IS5 and 50 μM insulin dramatically increases the inhibition of lipid-catalyzed kinetics (squares). Fits of the data to sigmoidal transitions are shown. Confidence intervals from triplicates are expressed in the text.

DISCUSSION

Oligopyridylamides represent a novel class of amyloid fiber formation effectors. Here, this class of compounds gives structurally specific insight into the processes of IAPP amyloid assembly. IS5 specifically inhibits fiber formation under lipid bilayer-catalyzed conditions. The in vivo potential for this approach is shown by IS5's ability to rescue IAPP-induced cytotoxicity. We show that this helix mimetic indeed binds to the helical region of IAPP. In the absence of a bilayer, stabilization of the helical region presumably results in structural rearrangements that accelerate aqueous phase nucleation. In the ER and/or granule lumen in vivo, IAPP is expressed in close proximity to insulin. Here, we have shown that IS5 can act synergistically with insulin to inhibit lipid-catalyzed fibrillogenesis.

The helical region of IAPP catalyzes amyloid nucleation. IS5 binds directly to the helical region of IAPP and accelerates de novo, solution phase fiber formation. Helical states of IAPP have been suggested to be important for kinetics both on liposomes and in solution. In the fiber state, IAPP forms in-register parallel β sheets (i.e., residue *i* of strand *j* stacks on top of residue *i* of strand *j* + *1*). This structural characteristic explains the insensitivity to primary sequence in some amyloid fibers. For example, Ure2p is able to form stable amyloid fibers even when its primary sequence is scrambled (Ross et al., 2004). In marked contrast, IAPP shows exquisite sensitivity to sequence order within its helical subdomain. The double mutants L12N/N14L and N14L/L16N have previously been shown to dramatically attenuate amyloid formation (Koo et al., 2008). Our data therefore support a model whereby the N-terminal helical region promotes formation of early intermediate states that allow β sheet formation to be initiated by some subset of the residues 20–37. This β sheet intermediate would then convert to the strand-loop-strand structure similar to the solid state NMR structure proposed by Luca et al. (2007) (Figure 1C). Inhibition by IS5 supports the direct assignment of helix-mediated nucleation as an element of the mechanism of IAPP fiber formation.

The presence of helix-based intermediates and the use of oligopyridylamide scaffolds holds the promise of creating highly specific attenuators of amyloid toxicity. Previous small molecule studies have relied on disruption of intermolecular contacts between β sheets. This mode of action explains the common ability for these classes of inhibitors to work in various amyloid systems (Porat et al., 2006). Other approaches take advantage of the 1D crystalline nature of amyloid fibers, using modified forms of the protein to disrupt amyloid formation. Such approaches are highly specific, but target fiber formation itself. The absence of any effect on elongation by IS5 indicates that it does not affect propagation of the amyloid structure (Figure 2B). It is therefore likely that N-terminal helix formation is not a feature of elongation. Plainly, IS5 is mechanistically distinct from the β sheet breaker or crystal poison class of small molecule inhibitors. Recent work has shown that libraries of thousands of helix mimetic compounds can be synthesized (Shaginian et al., 2009). This is afforded by the modular nature of the oligopyridylamide synthesis and will

facilitate structure-activity relationship studies for identifying promising drug candidates.

Inhibition by IS5 may further represent a type II diabetes-specific approach to compensate for loss of proteostasis control of IAPP by insulin. Proteostasis processes balance protein expression, localization, and degradation by enhancing folding and preventing misfolding through proper maintenance of chaperone levels. Restoring occurrences where this balance is lost would greatly aid the treatment of many diseases (Balch et al., 2008). Small molecules have been used to target improvements in homeostasis by two major avenues. First, target proteins can be stabilized by ligand binding, preventing misfolding and degradation. For example, the p53 mutant I195T can be stabilized by the peptide CDB3, which effectively acts as a synthetic chaperone (Friedler et al., 2002). Alternatively, celastrol and MG-132 have been used to upregulate core proteostasis machinery such as Hsp40 and Hsp70 (Mu et al., 2008). Upregulation of these core proteostasis proteins improves cell response to misfolding stress (Balch et al., 2008). These efforts show the importance of treating proteostasis machinery as a target for therapeutic intervention. Although insulin is not part of the unfolded protein response, it is cosecreted and coregulated with IAPP and is able to inhibit its fiber formation. Interestingly, insulin is a poor inhibitor of lipid-catalyzed IAPP fiber formation (Knight et al., 2008). We surmise that fiber formation in diabetes is an issue of localization. Lipid-bound IAPP is accessible to insulin (Knight et al., 2008) but does not form a structure with insulin that can effectively inhibit amyloidogenesis. Addition of IS5 partially rescues this effect and acts additively with insulin to inhibit amyloid formation. This restoration of native insulin inhibition may therefore represent a disease-specific opportunity to restore protein homeostasis and therefore prevent IAPP aggregation in type II diabetes.

SIGNIFICANCE

The oligopyridylamide IS5 interferes with lipid bilayer-bound states by targeting helical forms of IAPP. Our results clearly support the hypothesis that α-helical states are on pathway to β sheet fiber formation. More broadly, helical structure stabilized by lipid bilayers has been implicated in the mechanisms of other amyloid diseases including Aβ from Alzheimer's and α-synuclein from Parkinson's (Hebda and Miranker, 2009). For all three systems, there is interplay between structure formation, catalysis of fibrillogenesis, and cytotoxic loss of membrane integrity. In α-synuclein two helical states have been identified: one that is extended (Eliezer et al., 2001) and a second in which two helices are separated by a kink (Chandra et al., 2003). These alternative forms are suggested to have functional and/or pathological significance with respect to α-synuclein's ability to bind curved anionic vesicles. There are many suggested mechanisms for the origins of membrane integrity loss induced by these helical states. For example, Aβ can bind membranes in both lateral and transverse orientations (Bokvist et al., 2004; Chi et al., 2008). Subpeptide analyses have shown that IAPP helical states may behave similarly (Brender et al., 2008). It is therefore plausible that modulation between the two modes facilitates the depolarization of gradients across cellular membranes (Huang et al., 2004). Other suggested mechanisms include behavior that is detergent- and carpet-like and the direct formation of pores (Lashuel and Lansbury, 2006). This apparent range of possibility reveals the relative paucity of molecular level understanding. Specific targeting of helical, membrane-associated states using peptidomimetics will therefore enable the probing of these mechanisms through structure-activity relationships. This will further refine our ability to use mimetic compounds to target intermediates of amyloid rather than the fibers themselves. As IS5 rescues α-helical intermediate-induced cytotoxicity, such targeting represents a rich and novel area for the successful production of therapeutics.

SUPPLEMENTAL DATA

Supplemental Data include Supplemental Experimental Procedures and three figures and can be found with this article online at http://www.cell.com/chemistry-biology/supplemental/S1074-5521(09)00284-1.

ACKNOWLEDGMENTS

The authors thank J. Williamson and X. Wu for assistance with NMR; G. Cline and R. Pongratz for gift of INS-1 cells and assistance with cell culture; and J. Rodriguez, K. Tsou, and J. Becerril for assistance with synthesis. This work was supported by the National Institutes of Health National Institute of Diabetes and Digestive and Kidney Diseases grants DK079829 and AG031612 (to A.D.M.) and GM69850 (to A.D.H.).

Received: May 20, 2009
Revised: August 20, 2009
Accepted: August 27, 2009
Published: September 24, 2009

REFERENCES

Abedini, A., Meng, F., and Raleigh, D.P. (2007). A single-point mutation converts the highly amyloidogenic human islet amyloid polypeptide into a potent fibrillization inhibitor. J. Am. Chem. Soc. *129*, 11300–11301.

Aitken, J.F., Loomes, K.M., Konarkowska, B., and Cooper, G.J. (2003). Suppression by polycyclic compounds of the conversion of human amylin into insoluble amyloid. Biochem. J. *374*, 779–784.

Badman, M.K., Shennan, K.I., Jermany, J.L., Docherty, K., and Clark, A. (1996). Processing of pro-islet amyloid polypeptide (proIAPP) by the prohormone convertase PC2. FEBS Lett. *378*, 227–231.

Balch, W.E., Morimoto, R.I., Dillin, A., and Kelly, J.W. (2008). Adapting proteostasis for disease intervention. Science *319*, 916–919.

Bastianetto, S., Krantic, S., and Quirion, R. (2008). Polyphenols as potential inhibitors of amyloid aggregation and toxicity: possible significance to Alzheimer's disease. Mini Rev. Med. Chem. *8*, 429–435.

Bokvist, M., Lindstrom, F., Watts, A., and Grobner, G. (2004). Two types of Alzheimer's beta-amyloid (1-40) peptide membrane interactions: aggregation preventing transmembrane anchoring versus accelerated surface fibril formation. J. Mol. Biol. *335*, 1039–1049.

Brender, J.R., Lee, E.L., Cavitt, M.A., Gafni, A., Steel, D.G., and Ramamoorthy, A. (2008). Amyloid fiber formation and membrane disruption are separate processes localized in two distinct regions of IAPP, the type-2-diabetes-related peptide. J. Am. Chem. Soc. *130*, 6424–6429.

Chandra, S., Chen, X., Rizo, J., Jahn, R., and Sudhof, T.C. (2003). A broken alpha-helix in folded alpha-Synuclein. J. Biol. Chem. *278*, 15313–15318.

Chi, E.Y., Ege, C., Winans, A., Majewski, J., Wu, G., Kjaer, K., and Lee, K.Y. (2008). Lipid membrane templates the ordering and induces the fibrillogenesis of Alzheimer's disease amyloid-beta peptide. Proteins *72*, 1–24.

Clark, A., and Nilsson, M.R. (2004). Islet amyloid: a complication of islet dysfunction or an aetiological factor in Type 2 diabetes? Diabetologia *47*, 157–169.

Cooper, G.J. (1994). Amylin compared with calcitonin gene-related peptide: structure, biology, and relevance to metabolic disease. Endocr. Rev. *15*, 163–201.

Eliezer, D., Kutluay, E., Bussell, R., Jr., and Browne, G. (2001). Conformational properties of alpha-synuclein in its free and lipid-associated states. J. Mol. Biol. *307*, 1061–1073.

Findeis, M.A., Lee, J.J., Kelley, M., Wakefield, J.D., Zhang, M.H., Chin, J., Kubasek, W., and Molineaux, S.M. (2001). Characterization of cholyl-leu-val-phe-phe-ala-OH as an inhibitor of amyloid beta-peptide polymerization. Amyloid *8*, 231–241.

Finder, V.H., and Glockshuber, R. (2007). Amyloid-beta aggregation. Neurodegener. Dis. *4*, 13–27.

Frieden, C. (2007). Protein aggregation processes: In search of the mechanism. Protein Sci. *16*, 2334–2344.

Friedler, A., Hansson, L.O., Veprintsev, D.B., Freund, S.M., Rippin, T.M., Nikolova, P.V., Proctor, M.R., Rudiger, S., and Fersht, A.R. (2002). A peptide that binds and stabilizes p53 core domain: chaperone strategy for rescue of oncogenic mutants. Proc. Natl. Acad. Sci. USA *99*, 937–942.

Gong, Y., Chang, L., Viola, K.L., Lacor, P.N., Lambert, M.P., Finch, C.E., Krafft, G.A., and Klein, W.L. (2003). Alzheimer's disease-affected brain: presence of oligomeric A beta ligands (ADDLs) suggests a molecular basis for reversible memory loss. Proc. Natl. Acad. Sci. USA *100*, 10417–10422.

Grzesiek, S., Stahl, S.J., Wingfield, P.T., and Bax, A. (1996). The CD4 determinant for downregulation by HIV-1 Nef directly binds to Nef. Mapping of the Nef binding surface by NMR. Biochemistry *35*, 10256–10261.

Haataja, L., Gurlo, T., Huang, C.J., and Butler, P.C. (2008). Islet amyloid in type 2 diabetes, and the toxic oligomer hypothesis. Endocr. Rev. *29*, 303–316.

Harper, J.D., and Lansbury, P.T. (1997). Models of amyloid seeding in Alzheimer's disease and scrapie: mechanistic truths and physiological consequences of the time-dependent solubility of amyloid proteins. Annu. Rev. Biochem. *66*, 385–407.

Hay, D.L., Christopoulos, G., Christopoulos, A., and Sexton, P.M. (2004). Amylin receptors: molecular composition and pharmacology. Biochem. Soc. Trans. *32*, 865–867.

Hebda, J.A., and Miranker, A.D. (2009). The interplay of catalysis and toxicity by amyloid intermediates on lipid bilayers: insights form type II diabetes. Annu. Rev. Biophys. *38*, 125–152.

Hohmeier, H.E., Mulder, H., Chen, G., Henkel-Reiger, R., Prentki, M., and Newgard, C.B. (2000). Isolation of INS-1-derived cell lines with robust ATP-sensitive K+ channel-dependent and -independent glucose-stimulated insulin secretion. Diabetes *49*, 424–430.

Hoppener, J.W., Ahren, B., and Lips, C.J. (2000). Islet amyloid and type 2 diabetes mellitus. N. Engl. J. Med. *343*, 411–419.

Huang, H.W., Chen, F.Y., and Lee, M.T. (2004). Molecular mechanism of Peptide-induced pores in membranes. Phys. Rev. Lett. *92*, 198304.

Hull, R.L., Westermark, G.T., Westermark, P., and Kahn, S.E. (2004). Islet amyloid: a critical entity in the pathogenesis of type 2 diabetes. J. Clin. Endocrinol. Metab. *89*, 3629–3643.

Kahn, S.E., Andrikopoulos, S., and Verchere, C.B. (1999). Islet amyloid: a long-recognized but underappreciated pathological feature of type 2 diabetes. Diabetes *48*, 241–253.

Kayed, R., Sokolov, Y., Edmonds, B., McIntire, T.M., Milton, S.C., Hall, J.E., and Glabe, C.G. (2004). Permeabilization of lipid bilayers is a common conformation-dependent activity of soluble amyloid oligomers in protein misfolding diseases. J. Biol. Chem. *279*, 46363–46366.

Knight, J.D., and Miranker, A.D. (2004). Phospholipid catalysis of diabetic amyloid assembly. J. Mol. Biol. *341*, 1175–1187.

Knight, J.D., Hebda, J.A., and Miranker, A.D. (2006). Conserved and cooperative assembly of membrane-bound α-helical states of islet amyloid polypeptide. Biochemistry *45*, 9496–9508.

Knight, J.D., Williamson, J.A., and Miranker, A.D. (2008). Interaction of membrane-bound islet amyloid polypeptide with soluble and crystalline insulin. Protein Sci. *17*, 1850–1856.

Koo, B.W., Hebda, J.A., and Miranker, A.D. (2008). Amide inequivalence in the fibrillar assembly of islet amyloid polypeptide. Protein Eng. Des. Sel. *21*, 147–154.

Larson, J.L., and Miranker, A.D. (2004). The mechanism of insulin action on islet amyloid polypeptide fiber formation. J. Mol. Biol. *335*, 221–231.

Lashuel, H.A., and Lansbury, P.T. (2006). Are amyloid diseases caused by protein aggregates that mimic bacterial pore-forming toxins? Q. Rev. Biophys. *39*, 167–201.

LeVine, H. (2007). Small molecule inhibitors of Abeta assembly. Amyloid *14*, 185–197.

Luca, S., Yau, W.M., Leapman, R., and Tycko, R. (2007). Peptide conformation and supramolecular organization in amylin fibrils: constraints from solid-state NMR. Biochemistry *46*, 13505–13522.

Marzban, L., Park, K., and Verchere, C.B. (2003). Islet amyloid polypeptide and type 2 diabetes. Exp. Gerontol. *38*, 347–351.

Matveyenko, A.V., and Butler, P.C. (2006a). Beta-cell deficit due to increased apoptosis in the human islet amyloid polypeptide transgenic (HIP) rat recapitulates the metabolic defects present in type 2 diabetes. Diabetes *55*, 2106–2114.

Matveyenko, A.V., and Butler, P.C. (2006b). Islet amyloid polypeptide (IAPP) transgenic rodents as models for type 2 diabetes. ILAR J. *47*, 225–233.

Mu, T.W., Ong, D.S., Wang, Y.J., Balch, W.E., Yates, J.R., Segatori, L., and Kelly, J.W. (2008). Chemical and biological approaches synergize to ameliorate protein-folding diseases. Cell *134*, 769–781.

Padrick, S.B., and Miranker, A.D. (2002). Islet amyloid: phase partitioning and secondary nucleation are central to the mechanism of fibrillogenesis. Biochemistry *41*, 4694–4703.

Pontiroli, A.E. (2004). Type 2 diabetes mellitus is becoming the most common type of diabetes in school children. Acta Diabetol. *41*, 85–90.

Porat, Y., Mazor, Y., Efrat, S., and Gazit, E. (2004). Inhibition of islet amyloid polypeptide fibril formation: a potential role for heteroaromatic interactions. Biochemistry *43*, 14454–14462.

Porat, Y., Abramowitz, A., and Gazit, E. (2006). Inhibition of amyloid fibril formation by polyphenols: structural similarity and aromatic interactions as a common inhibition mechanism. Chem. Biol. Drug Des. *67*, 27–37.

Porte, D., Jr., and Kahn, S.E. (2001). beta-cell dysfunction and failure in type 2 diabetes: potential mechanisms. Diabetes *50 Suppl 1*, S160–S163.

Powers, E.T., and Powers, D.L. (2008). Mechanisms of protein fibril formation: nucleated polymerization with competing off-pathway aggregation. Biophys. J. *94*, 379–391.

Rao, J.N., Dua, V., and Ulmer, T.S. (2008). Characterization of alpha-synuclein interactions with selected aggregation-inhibiting small molecules. Biochemistry *47*, 4651–4656.

Ross, E.D., Baxa, U., and Wickner, R.B. (2004). Scrambled prion domains form prions and amyloid. Mol. Cell. Biol. *24*, 7206–7213.

Ruschak, A.M., and Miranker, A.D. (2007). Fiber-dependent amyloid formation as catalysis of an existing reaction pathway. Proc. Natl. Acad. Sci. USA *104*, 12341–12346.

Saraogi, I., and Hamilton, A.D. (2008). alpha-Helix mimetics as inhibitors of protein-protein interactions. Biochem. Soc. Trans. *36*, 1414–1417.

Saraogi, I., Hebda, J.A., Becerril, J., Estroff, L.A., Miranker, A.D., and Hamilton, A.D. (2009). Synthetic alpha-helix mimetics as agonists and antagonists of IAPP amyloid formation. Angew. Chem. Int. Ed. Engl, in press. 10.1003/anie.200901694.

Shaginian, A., Whitby, L.R., Hong, S., Hwang, I., Farooqi, B., Searcey, M., Chen, J., Vogt, P.K., and Boger, D.L. (2009). Design, synthesis, and evaluation

of an alpha-helix mimetic library targeting protein-protein interactions. J. Am. Chem. Soc. *131*, 5564–5572.

Tycko, R. (2006). Molecular structure of amyloid fibrils: insights from solid-state NMR. Q. Rev. Biophys. *39*, 1–55.

Wang, H., Duennwald, M.L., Roberts, B.E., Rozeboom, L.M., Zhang, Y.L., Steele, A.D., Krishnan, R., Su, L.J., Griffin, D., Mukhopadhyay, S., et al. (2008). Direct and selective elimination of specific prions and amyloids by 4,5-dianilinophthalimide and analogs. Proc. Natl. Acad. Sci. USA *105*, 7159–7164.

Williamson, J.A., and Miranker, A.D. (2007). Direct detection of transient α-helical states in islet amyloid polypeptide. Protein Sci. *16*, 110–117.

Yan, L.M., Tatarek-Nossol, M., Velkova, A., Kazantzis, A., and Kapurniotu, A. (2006). Design of a mimic of nonamyloidogenic and bioactive human islet amyloid polypeptide (IAPP) as nanomolar affinity inhibitor of IAPP cytotoxic fibrillogenesis. Proc. Natl. Acad. Sci. USA *103*, 2046–2051.

